ELSEVIER

Ultrasonics 37 (1999) 355–363

Ultrasonics

www.elsevier.nl/locate/ultras

Guided waves by axisymmetric and non-axisymmetric surface loading on hollow cylinders

Hyeon Jae Shin, Joseph L. Rose *

Department of Engineering Science and Mechanics, The Pennsylvania State University, 114 Hallowell Bldg, University Park, PA 16801, USA

Received 14 December 1998

Abstract

Guided waves generated by axisymmetric and non-axisymmetric surface loading on a hollow cylinder are studied. For the theoretical analysis of the superposed guided waves, a normal mode concept is employed. The amplitude factors of individual guided wave modes are studied with respect to varying surface pressure loading profiles. Both theoretical and experimental focus is given to the guided waves generated by both axisymmetric and non-axisymmetric excitation. For the experiments, a comb transducer and high power tone burst function generator system are used on a sample Inconel tube. Surface loading conditions, such as circumferential loading angles and axial loading lengths, are used with the frequency and phase velocity to control the axisymmetric and non-axisymmetric mode excitations. The experimental study demonstrates the use of a practical non-axisymmetric partial loading technique in generating axisymmetric modes, particularly useful in the inspection of tubing and piping with limited circumferential access. From both theoretical and experimental studies, it also could be said that the amount of flexural modes reflected from a defect contains information on the reflector's circumferential angle, as well as potentially other classification and sizing feature information. The axisymmetric and non-axisymmetric guided wave modes should both be carefully considered for improvement of the overall analysis of guided waves generated in hollow cylinders.

Keywords: Dispersion curves; Flexural modes; Guided waves; Hollow cylinders; Non-axisymmetric

1. Introduction

Guided waves are associated with acoustic wave propagation in wave-guides. Tubing and piping structures are excellent wave-guides. The benefits of using ultrasonic guided waves in our large infrastructure inspections are cost effectiveness, time efficiency, and improved sensitivity using multiple guided wave modes. Especially in tubing and piping evaluation, there are many guided wave modes that can be used to evaluate an entire cross-sectional area as well as a long length of the structure with just one probe position, even without any probe rotation. Guided waves propagate over curved sections, as well as in straight sections of tubing. Improved inspection speed and minimal probe movements provide major benefits compared with existing techniques that rely on point-by-point and rotating probes for inspections. Ultrasonic guided waves also can be used for both ferromagnetic and non-ferromagnetic materials with various boundary conditions, such as traction free, coatings, insulations, and water loading. Therefore, applications of ultrasonic guided waves are countless in the field of materials evaluation and safety monitoring.

The subject of guided waves in a hollow cylinder has been studied for many years. The general solution of harmonic wave propagation in an infinitely long elastic hollow cylinder has been obtained by Gazis [1,2] using elasticity theory. Also, Greenspon [3,4] studied the theory of elasticity independently and published some of the dispersion curves and displacement fields for a cylindrical shell. Fitch [5] experimentally studied guided waves for delay-line applications. As industry calls for advanced non-destructive evaluation techniques for tubing and piping structures, feasibility studies on guided waves for defect detection in hollow cylinders were initiated. In 1979, Thompson et al. [6] introduced an EMAT system for the detection of flaws in steam generator tubes. For the generation of ultrasonic guided waves in heat exchanger tubing, Silk and Bainton [7] investigated piezoelectric ultrasonic probes for access to

* Corresponding author. Tel.: +1-814-863-8026; fax: +1-814-863-8164.
E-mail address: jlresm@engr.psu.edu (J.L. Rose)

0041-624X/99/$ – see front matter
PII: S0041-624X(99)00010-4

the inside of the tube. They also tried to detect flaws and to show the possibility of using guided waves in tubing inspection. Brook et al. [8] demonstrated the feasibility of using cylindrical guided wave modes for the inspection of steam generator tubing by normal beam transmission from the end of the tube. It is interesting to see that Silk and Bainton [7] used the L(0, 1) mode, but that Brook et al. [8] used the L(0, 2) mode. Brook et al. [8] generated strong L(0, 2) modes but a weak L(0, 1) mode. L(0, 1) corresponds to A_0 and L(0, 2) corresponds to S_0 in the paper. This contradiction results from the different guided wave excitation methods. Silk and Bainton [7] excited guided waves from the inside of the tube, whereas Brook et al. [8] did it from the cross-section of the tube end. These experiments demonstrated the utility of guided waves in tubing inspection, but left much space to achieve real field application.

Great progress has been demonstrated in the utility of axisymmetric longitudinal guided wave modes for tubing inspection. Ditri and coworkers [9–11] introduced improved tubing inspection concepts and listed many theoretical and practical considerations. They discussed the phase and group velocity dispersion curves, and introduced the acoustic field distribution across the tube wall thickness, the so-called 'wave structure curves'. A list of mode selection and generation concepts including special designs of guided wave transducers, such as angle beam wedges and comb, were also introduced. Rose and coworkers [12–14] introduced wave structure curves for steam generator tubing and discussed mode selection concepts including excellent defect detection results. They also presented experimental results for leaky and non-leaky guided wave modes in tubing, and explained the results based on the wave structure curves. Alleyne et al. [15,16] suggested the use of the fastest mode in a non-dispersive region of the frequency range, to use single modes in avoiding the complexity of multiple mode propagation and mode conversions, and presented an experimental study of the excitation of guided waves in piping. For a physical understanding of the guided wave excitation in hollow cylinders, Ditri and Rose [17] published a paper entitled "Excitation of guided wave modes in hollow cylinders by applied surface tractions". In that paper, they employed the normal mode expansion amplitude method for the theoretical predictions of the acoustic field distributions along hollow cylinders due to arbitrary boundary loading conditions.

Very little work effort is reported on non-axisymmetric guided waves in tubing and piping. In hollow cylinders, non-axisymmetric modes are also called 'flexural modes'. Shin and Rose [18] used a non-axisymmetric partial loading transducer setup to generate non-axisymmetric guided waves in tubing, and introduced tuning concepts that demonstrated the possibility of inspecting an entire cross-sectional area, as well as a long length of a tube. The generated guided waves by non-axisymmetric partial loading on the sample tube are superpositions of a multiple number of guided wave modes. The study also shows a promising utility of guided waves excited by non-axisymmetric partial loading on tubing and piping that have limited access to the circumference.

Based on previous studies and experimental experience, there are strong reasons for studying complex non-axisymmetric guided waves. (1) Non-axisymmetric reflections occur, even for axisymmetric impingement because of non-axisymmetric reflectors. (2) There are mode conversions among the axisymmetric and non-axisymmetric modes. (3) Unusual effects are still often found in attempts at using axisymmetric modes. (4) It is hard to generate a single axisymmetric mode in a certain frequency range. (5) For certain kinds of transverse, angular or axial defects, non-axisymmetric wave modes could be more efficient than axisymmetric modes. (6) Limited access to the inspected sample often requires inevitable non-axisymmetric loading conditions. (7) Besides these practical reasons, it is also very interesting to explore the acoustic characteristics of guided waves excited by various non-axisymmetric loading conditions.

In this paper, guided waves generated by axisymmetric and non-axisymmetric surface pressure loadings on a hollow cylinder are studied. It is assumed that the superposition of individual guided wave modes results in a non-axisymmetric guided wave. For the theoretical analysis of the superimposed guided waves, a normal mode summation concept is employed. The amplitude factors of the individual guided wave modes are discussed with respect to varying surface pressure loading. For the source design parameters, the applied loading length and circumferential angle are considered. Theoretical and experimental attention is given to the guided waves generated by axisymmetric and non-axisymmetric excitation. For the experiments, a comb transducer and high power tone burst function generator system are used on a sample Inconel tube.

2. Guided wave modes and the superposition of normal modes

There is an infinite number of guided wave modes in a cylindrical waveguide. Finding and sorting the best modes for an inspection, therefore, represents a necessary step towards understanding guided wave propagation and scattering for inspection sensitivity. Two indices, circumferential order M and mode number n, are used to describe guided wave modes in tubing. In tubing or piping, three types of mode are described: longitudinal, torsional, and flexural. All of these guided wave modes propagate in the axial direction of a cylin-

drical waveguide. When $M=0$, the acoustic fields of the modes are axisymmetric along a cylinder circumference. Otherwise, the modes are non-axisymmetric. Longitudinal modes, $L(0,n)$, and torsional modes, $T(0,n)$, are axisymmetric, and the flexural modes, $F(M,n)$, represent the non-axisymmetric modes.

In guided wave propagation in tubing, the phase velocity is usually different from the energy traveling velocity, i.e. group velocity in assumed lossless media. Both phase and group velocities vary with both tubing thickness and frequency. Therefore, the dispersive character and subsequent frequency dependence of the guided wave must be studied. From a practical point of view, it is convenient to represent the velocities in terms of a frequency times the thickness fd of the waveguide, which then leads to the traditional phase or group velocity dispersion diagram [18,19]. Fig. 1 shows a sample set of (a) phase and (b) group velocity dispersion curves for an Inconel tube with traction-free boundary conditions. Some of the longitudinal modes, $L(0,n)$, and flexural modes, $F(M,n)$, are shown in these dispersion diagrams. Material properties and dimensions of the Inconel tube are given in Table 1. Inconel tubing is a key component in the nuclear power industry. As shown in Fig. 1, it is possible to have a multiple number of guided wave modes at a constant frequency, but all with different velocities. The total number of guided wave modes for a given fd value is countable and increases as frequency gets higher.

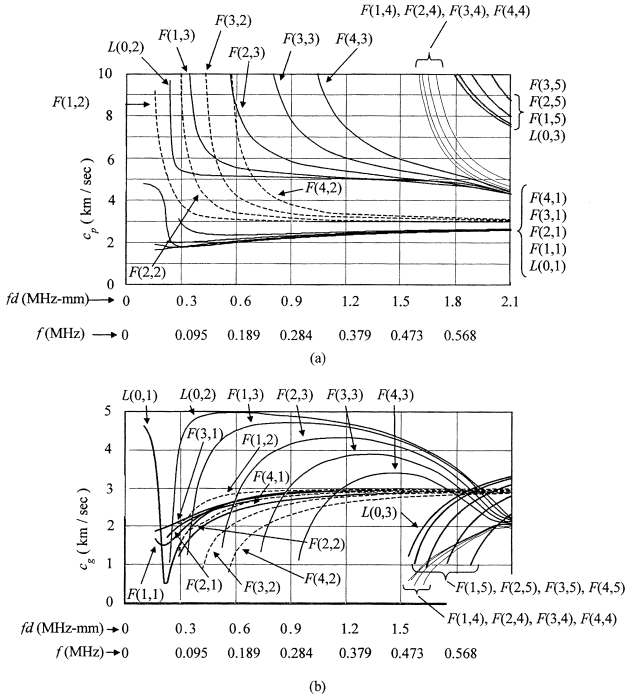

Fig. 1. Dispersion diagrams for the sample Inconel tube showing some longitudinal and flexural modes. (a) Phase velocity dispersion diagram. (b) Group velocity dispersion diagram.

The acoustic character of each mode at a particular frequency is different. The acoustic character can be considered as varying with the change of the fd value along a given mode. The varying acoustic character results from such acoustic field variables as polarization and amplitude of the particle vibration. The acoustic fields are non-uniform across the thickness of a waveguide, except in a few special cases.

Generation of guided wave modes of choice and possible isolation is one of the key theoretical and experimental challenges in guided wave experiments. Axisymmetric excitation within a selected frequency band range could generate a well-defined guided wave packet in the time domain. A well-defined guided wave packet is useful because of easy identification of the received guided wave modes and also for inspection sensitivity. A well-defined wave packet is composed of guided wave modes with close and/or identical phase velocities. This usually happens within a same mode or a group of modes converging on a special group velocity value. Non-axisymmetric excitation often leads to a number of guided wave modes. In this case, it is quite difficult to produce a well-defined guided wave packet to compare with an axisymmetric excitation result.

Superposition concepts are suitable for examining the contribution of each individual mode to the final guided wave formation. Amplitudes of each individual mode can be calculated by using the normal mode expansion method, which is then used to a final acoustic field with a superposition of a complete set of guided wave modes [17,20]. For example, the final particle velocity field can be expanded as a superposition of normal modes traveling in a waveguide, and can be written as

$$\boldsymbol{v}\,\mathrm{e}^{\mathrm{i}\omega t}=\sum_{M,n}A_n^M\boldsymbol{v}_n^M\,\mathrm{e}^{\mathrm{i}(\omega t)} \tag{1}$$

where ω is an angular frequency. A_n^M is a normal mode expansion amplitude that includes the term $\mathrm{e}^{\mathrm{i}(-k_n^M z)}$. For a given frequency, $\boldsymbol{v}_n^M$ is a velocity field of the nth mode of Mth circumferential order, and can be written in a cylindrical coordinate system as follows:

$$\begin{aligned}\boldsymbol{v}_n^M(r,\theta)=R_n^M(r)\cdot\Theta^M(\theta)&=\mathrm{i}R_{nr}^M(r)\Theta_r^M(M\theta)\boldsymbol{e}_r\\&\quad+\mathrm{i}R_{n\theta}^M(r)\Theta_\theta^M(M\theta)\boldsymbol{e}_\theta\\&\quad+R_{nz}^M(r)\Theta_z^M(M\theta)\boldsymbol{e}_z\end{aligned} \tag{2}$$

where $\mathrm{i}=\sqrt{-1}$. The range of r is between the inner and outer radius of a cylinder. Note that the velocity field for a mode at a given frequency is independent of the axial position in a cylinder. $R_n^M(r)$ represents a radial component of particle velocity determined by a radial position within the thickness of a cylinder. $R_n^M(r)$ represents a combination of Bessel functions and modified Bessel functions [19]. $\Theta^M(\theta)$ represents an angular component of particle velocity determined by an angular position. $\Theta^M(\theta)$ consists of sinusoidal functions having

Table 1
Material properties and dimensions of a sample Inconel tube

Length (mm)	609.6
Outer diameter (mm)	25.4
Thickness (mm)	3.17
Longitudinal velocity (km/s)	5.7
Transverse velocity (km/s)	3.0

an argument of $M\theta$. For $M=0$, $\Theta_r^M(M\theta)=0$ or 1, and the guided wave modes will be axisymmetric as mentioned before. For $M=1, 2, 3 \ldots$, the guided wave modes are non-axisymmetric, flexural modes, indicated as $F(M, n)$.

For example, $\Theta_r^M(M\theta)$ can be represented by $\cos(M\theta)$. Fig. 2 shows sample acoustic fields for different circumferential orders M along a hollow cylinder circumference.

With the traction-free boundary conditions on the inner boundary $\partial_1 D$ and the outer boundary $\partial_2 D$ of the hollow elastic cylinder, the general form of the forward propagating normal mode expansion amplitude for the traction free hollow cylinder will be

$$A_{+n}^M(z)=\frac{e^{-ik_n^M z}}{4P_{nn}^{MM}}\int_c^z e^{ik_n^M \eta} \times\left[\oint_{\partial_1 D} \boldsymbol{v}_n^{M*}\cdot(\boldsymbol{T}\cdot\boldsymbol{n}_1)\,ds+\oint_{\partial_2 D} \boldsymbol{v}_n^{M*}\cdot(\boldsymbol{T}\cdot\boldsymbol{n}_2)\,ds\right]d\eta \quad (3)$$

where the lower and upper limits c and z will be determined to satisfy the boundary conditions [17]. The asterisk indicates complex conjugation. The terms, $(\boldsymbol{T}\cdot\boldsymbol{n}_1)$ and $(\boldsymbol{T}\cdot\boldsymbol{n}_2)$, are the loading (source) conditions on the inner and outer boundaries of the hollow cylinder, where $\boldsymbol{n}_1$ and $\boldsymbol{n}_2$ are the unit normal vectors pointing away from the inner boundary and the outer boundary, respectively. P_{nn}^{MM} is a power carried by an nth mode of Mth circumferential order.

3. Applied surface pressure and guided wave modes in a hollow cylinder

Let us assume that a hollow elastic cylinder is loaded only on the outer boundary and an applied traction is

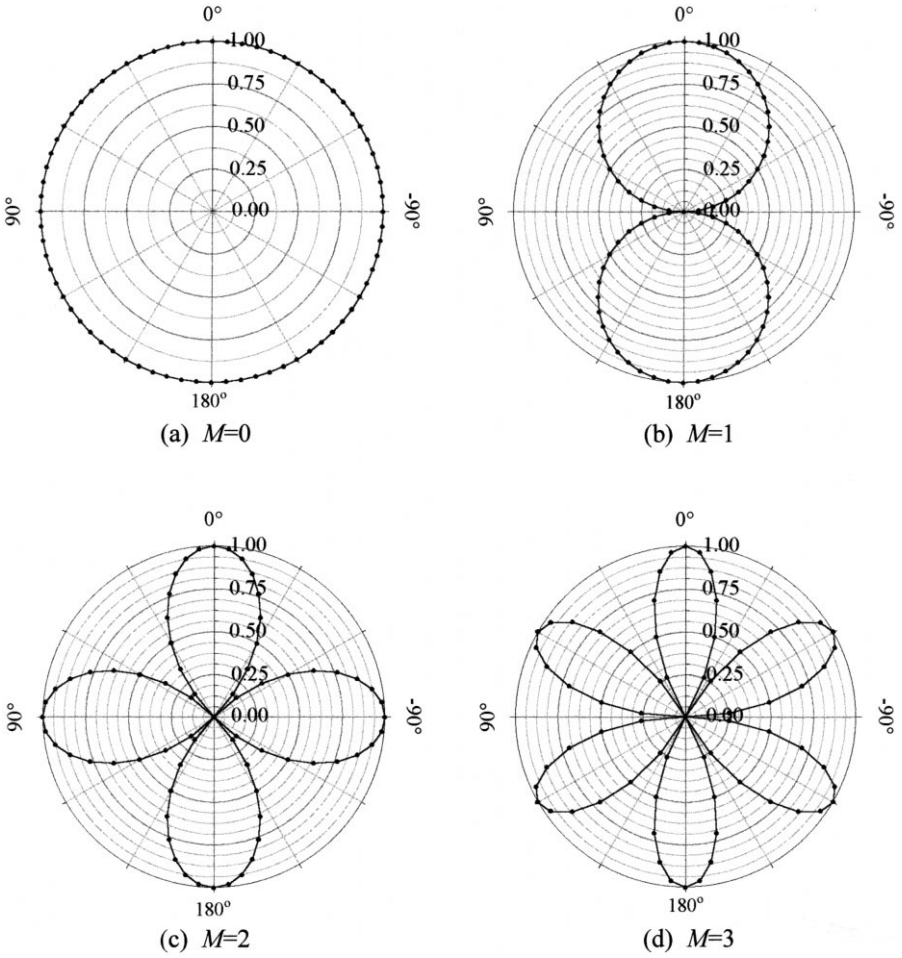

Fig. 2. Circumferential order and amplitude distributions for the radial components of particle velocities of guided waves in hollow cylinders.

a pressure loading applied to the negative radial direction, as shown in Fig. 3. The term $-p\boldsymbol{e}_r$ can be represented by $-p_1(\theta)p_2(z)$. The inner and outer radius are a and b respectively. $2L$ is an applied loading length and α is an applied circumferential loading angle. $\boldsymbol{e}_z$, $\boldsymbol{e}_r$, and $\boldsymbol{e}_\theta$ are unit normal vectors in a cylinder coordinate system. In Eq. (3)

$$\boldsymbol{T}\cdot\boldsymbol{n}_1=0 \tag{4}$$

$$\boldsymbol{T}\cdot\boldsymbol{n}_2=-p_1(\theta)p_2(z)\boldsymbol{e}_r \text{ for } |z|\le L \text{ and } |\theta|<\alpha/2,\ r=b$$

$$\boldsymbol{T}\cdot\boldsymbol{n}_2=0 \text{ for } |z|>L \text{ or } |\theta|>\alpha/2,\ r=b. \tag{5}$$

Substituting Eqs. (4) and (5) into Eq. (3) gives

$$A^M_{+n}(z)=\mathrm{e}^{-\mathrm{i}k^M_n z}\,\frac{R^{M*}_{nr}(b)}{4P^{MM}_{nn}}\,\langle\Theta^M_r,p_1(\theta)\rangle\langle p_2(z),\mathrm{e}^{\mathrm{i}k^M_n z}\rangle,\ z\ge L \tag{6}$$

where

$$\langle\Theta^M_r,p_1(\theta)\rangle\equiv b\int_{\theta_0}^{\theta_0+2\pi}\Theta^M_r(\theta)p_1(\theta)\,\mathrm{d}\theta \tag{7}$$

$$\langle p_2(z),\mathrm{e}^{\mathrm{i}k^M_n z}\rangle\equiv\int_{-\infty}^{\infty}p_2(z)\,\mathrm{e}^{\mathrm{i}k^M_n z}\,\mathrm{d}z. \tag{8}$$

The term $R^{M*}_{nr}(b)/(4P^{MM}_{nn})$ in Eq. (6) is an amplitude factor that represents the excitability of the nth mode of Mth circumferential order in this outer surface loading condition. $R^{M*}_{nr}(b)$ is the radial component of particle velocity at the outer surface of the tubing. For torsional modes $|R^{M*}_{nr}(b)|=0$, and the normal mode expansion amplitude is zero in this surface pressure loading condition, regardless of the source geometry. For longitudinal and flexural modes, $|R^{M*}_{nr}(b)|$ varies with frequencies as well as the particular modes. Therefore, this surface pressure loading will excite longitudinal modes and/or flexural modes depending on the applied pressure distributions on the tube surface. The terms $\langle\Theta^M_r,p_1(\theta)\rangle$ and $\langle p_2(z),\mathrm{e}^{\mathrm{i}k^M_n z}\rangle$ are amplitude factors depending on such source parameters as pressure distribution, coupling condition, and source geometry.

The circumferential amplitude factor $\langle\Theta^M_r,p_1(\theta)\rangle$ is determined by the circumferential pressure distribution applied on a cylinder. $\Theta^M_r(M\theta)$ can be represented by $\cos(M\theta)$. For a uniform pressure loading condition, $p_1(\theta)$ is a constant, P_{10}, and the circumferential amplitude factor will then be

$$\langle\Theta^M_r,p_1(\theta)\rangle=b\int_{-\alpha/2}^{\alpha/2}\Theta^M_r(\theta)P_{10}\,\mathrm{d}\theta=bP_{10}\alpha,\ \text{for } M=0 \tag{9}$$

$$\langle\Theta^M_r,p_1(\theta)\rangle=b\int_{-\alpha/2}^{\alpha/2}\Theta^M_r(\theta)P_{10}\,\mathrm{d}\theta=2(bP_{10})\,\frac{\sin[(\alpha/2)M]}{M},\ \text{for } M\ge1.$$

$M=0$ is for the axisymmetric mode and $M\ge0$ are for the non-axisymmetric modes. There is a linear relationship between the circumferential amplitude factor and the amplitude of the applied pressure. There is also a linear relationship between the axisymmetric circumferential amplitude factor and loading angle α. The relationship is also independent of phase velocity and frequency and is a function of α and M. The relative circumferential amplitude factor with respect to the factor of the axisymmetric longitudinal mode can be written as

$$\frac{\langle\Theta^M_r,p_1(\theta)\rangle}{\langle\Theta^0_r,p_1(\theta)\rangle}=1,\ \text{for } M=0$$

$$\frac{\langle\Theta^M_r,p_1(\theta)\rangle}{\langle\Theta^0_r,p_1(\theta)\rangle}=\frac{2\sin[(\alpha/2)M]}{\alpha M},\ \text{for } M\ge1. \tag{10}$$

Fig. 4 shows relative circumferential amplitude factors for different applied surface loading angles of $\alpha=360^\circ$, $\alpha=180^\circ$, $\alpha=90^\circ$, and $\alpha=45^\circ$. Negative amplitude represents phase change. For an axisymmetric loading, $\alpha=360^\circ$, all of the amplitude factors are zero as expected, except for the axisymmetric modes. For 180° applied surface loading there is still a dominant axisymmetric mode compared with the flexural modes. As the loading angle decreases, however, the chance of flexural mode generation increases.

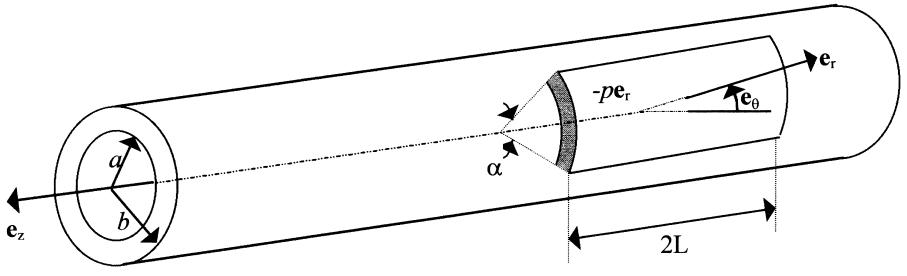

Fig. 3. The hollow cylinder with a pressure loading, $-p\boldsymbol{e}_r$, on the outer boundary $\partial_2 D$. The inner and outer radius are a and b respectively. $\boldsymbol{e}_z$, $\boldsymbol{e}_r$, and $\boldsymbol{e}_\theta$ are unit normal vectors.

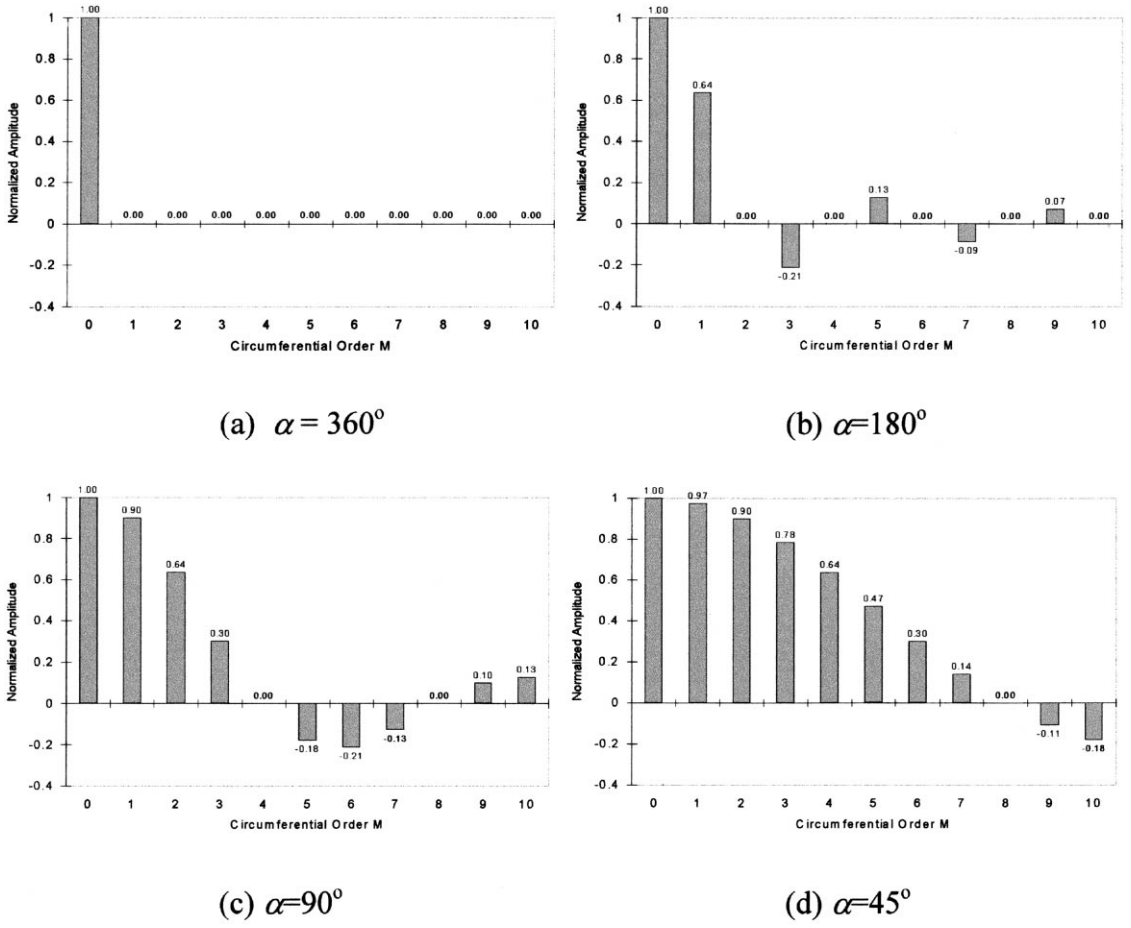

Fig. 4. Relative circumferential amplitude factors for axisymmetric modes ($M=0$) and flexural modes ($M\geq 1$) at various loading angles: (a) $\alpha=360^\circ$; (b) $\alpha=180^\circ$; (c) $\alpha=90^\circ$; (d) $\alpha=45^\circ$.

The axial amplitude factor $\langle p_2(z), e^{ik_n^M z}\rangle$ is determined by the axial pressure distribution applied on the cylinder. Let us assume that the applied loading length is $2L$, and $p_2(z)$ is a constant P_{20}, a uniform pressure loading condition; the axial amplitude field will then be

$$\langle p_2(z), e^{ik_n^M z}\rangle = \int_{-L}^{L} p_2(z)\, e^{ik_n^M z}\, dz = \frac{2P_{20}}{k_n^M}\sin(k_n^M L) \text{ for } z\geq L. \quad (11)$$

There is also a linear relationship between the axial amplitude factor and the amplitude of the applied pressure. The relative axial amplitude factor can be written as

$$\frac{\langle p_2(z), e^{ik_n^M z}\rangle}{2P_{20}/k_n^0} = \sin(k_n^0 L) \text{ for } M=0$$
$$\frac{\langle p_2(z), e^{ik_n^M z}\rangle}{2P_{20}/k_n^0} = \frac{\sin(k_n^M L)k_n^0}{k_n^M} \text{ for } M\geq 1. \quad (12)$$

It is dependent on wave number k_n^M. Therefore, the axial amplitude factor is a function of phase velocity and frequency as well as axial pressure loading length, $2L$. This factor will be maximum when $k_n^M L=\pi(q+\frac{1}{2})$ where $q=0, 1, 2, 3$ …. Therefore, the efficient axial loading length for a mode at a particular frequency will be

$$2L=\lambda_n^M(q+\tfrac{1}{2}) \quad (13)$$

where $\lambda_n^M$is the wavelength. For a given frequency, a phase velocity value of a guided wave mode of choice is found on a phase velocity dispersion diagram. The optimum surface pressure loading length, $2L$, will be found by Eq. (13) for the generation of the selected mode. Therefore, controlling guided wave modes in tubing will be possible by means of controlling the length of the uniform axial surface pressure, as shown in Fig. 3. For a fixed frequency, there are countable numbers of guided wave modes that have different phase velocities, as shown in Fig. 1. Fig. 5 shows sample axial amplitude factor variations due to varying surface pressure loading lengths for L(0, 2) and F(3, 3) at an *fd* value of 1.2 MHz mm in the sample Inconel tube. Phase velocities for L(0, 2) and F(3, 3) at 1.2 MHz mm are 5 km/s and 6 km/s respectively. The first maximum of the factor occurs at 6.6 mm for L(0, 2) and 7.9 mm for

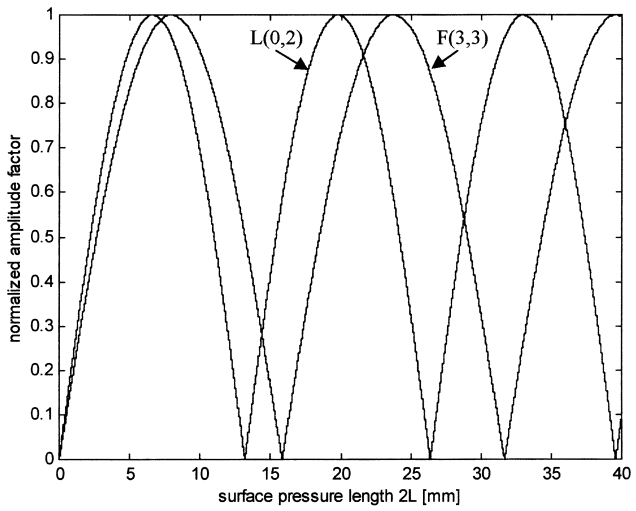

Fig. 5. The axial amplitude factor variations due to varying surface pressure loading lengths for L(0, 2) and F(3, 3) at an *fd* value of 1.2 MHz mm in the sample Inconel tube. Phase velocity for L(0, 2) and F(3, 3) at 1.2 MHz mm are 5 km/s and 6 km/s respectively. The first maximum of the factor occurs at 6.6 mm for L(0, 2) and 7.9 mm for F(3, 3).

F(3, 3). Therefore, optimum source lengths are found for the excitation of selected modes. The length at the third maximum in L(0, 2) is optimized for the generation of L(0, 2) effectively, while depressing F(3, 3).

4. A circumferential angle guided wave experiment

The experimental study presented here focuses on an observation of guided waves generated in tubing by a comb transducer with a changing circumferential loading angle. It is intriguing to consider transmitted non-axisymmetric waves as well as axisymmetric waves, primarily because of the simplicity in generation and often practical limitations of limited access to the total circumference. In this case, it is very advantageous to know the relationship between the circumferential loading angle and the types of generated guided wave. These experiments will also prove that the trends predicted by the theoretical results shown in Fig. 4 are correct.

In these experiments, the Inconel tube shown in Table 1 was used. A pair of 180° comb transducers was fabricated to fit over the outer surface of the tube. The transducers were placed at one end of the tube and the pulse echo technique was used with coupling windows to control the applied loading angle. Coupling windows allow ultrasonic wave propagation from the transducer to the Inconel tube. Selected loading angles were $\alpha = 360°$, $\alpha = 180°$, $\alpha = 90°$, and $\alpha = 45°$. Eight cycles of a tone burst signal at 0.395 MHz, corresponding to an *fd* value of 1.25 MHz mm in the dispersion curves shown in Fig. 1, were excited by a tone burst function generator system. Since there were no flaws in the tube, the only reflections that occurred, therefore, were from the tube end. Modes around the *fd* value of 1.25 MHz mm were studied, since the L(0, 2) modes at that frequency had good penetration and defect detection. Because of the phase velocity and frequency spectrum bandwidths, excitation occurs over an area centered at an *fd* value of 1.25 MHz mm and a phase velocity of 5 km/s as obtained from the dispersion diagram in Fig. 1. The theoretically estimated group velocity of L(0, 2) at the *fd* value of 1.25 MHz mm was about 4.75 km/s.

Fig. 6 shows guided wave pulse echo results on the sample Inconel tube for various circumferential loading angles, including (a) $\alpha = 360°$, (b) $\alpha = 180°$, (c) $\alpha = 90°$, and (d) $\alpha = 45°$. For 360° axisymmetric loading, successive echoes of a strong and isolated mode were observed. Successive echoes are due to guided waves bouncing between tube ends. Four successive back wall echoes are shown. Excellent penetration ability is obtained. The gain required to saturate the first back wall echo was 37.5 dB. An experimentally measured group velocity was 5.0 km/s. This mode corresponds to the longitudinal mode L(0, 2). In a realistic test situation, this mode would be useful for a quick screening test over long distances of the tubing without moving the transducer. For the circumferential loading angle of 180°, in Fig. 6(b), the generation of the L(0, 2) mode was still very dominant. Note the presence of small flexural mode components between the subsequent axisymmetric tube end echoes. This shows, however, that a 180° partial loading situation could indeed generate an acceptable axisymmetric mode for tubing inspection with this excitation method. Modes followed by the L(0, 2) mode correspond to some flexural modes or a superposition of a number of guided wave modes having slower group velocities compared with L(0, 2). As the loading angles decrease to 90° and 45°, Fig. 6(c) and (d), the presence of flexural modes gets large. In these cases, there are many modes, and the signal-to-noise ratio with the axisymmetric mode as reference would not be good for defect detection analysis.

These experimental results clearly demonstrate the trend that was predicted by the theoretical results shown in Fig. 4. One more significant observation is that the amount of flexural mode presence could possibly tell us about the circumferential extent of a defect. Whenever an axisymmetric mode hits a flaw in a hollow cylinder, the flaw will be a virtual source of a guided wave generation as a result of reflection and scattering. The amount of flexural mode content in the reflected signals would be closely related to the circumferential extent of the flaw.

5. Concluding remarks

An understanding of both axisymmetric and non-axisymmetric guided wave mode propagation in hollow

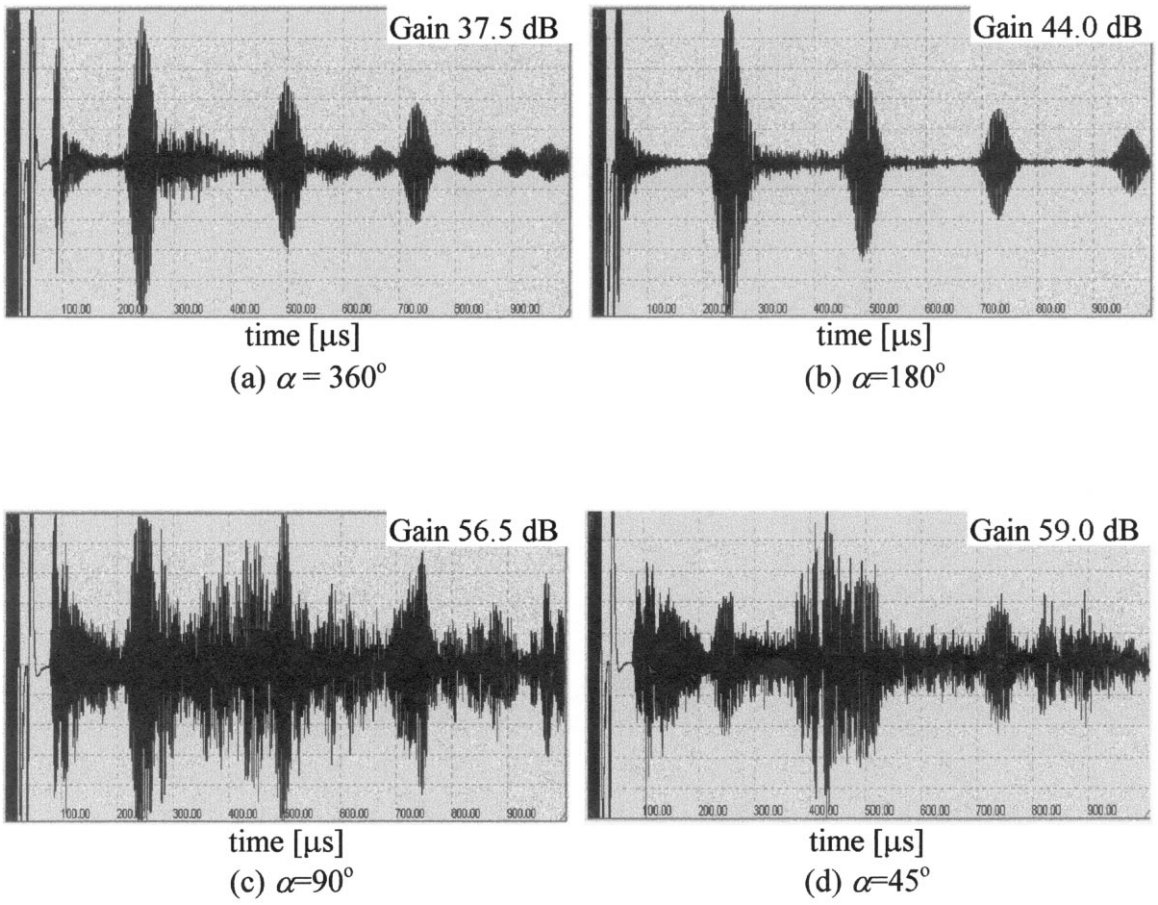

Fig. 6. Guided wave pulse echo results on a sample Inconel tube for various circumferential loading angles: (a) $\alpha = 360^\circ$; (b) $\alpha = 180^\circ$; (c) $\alpha = 90^\circ$; (d) $\alpha = 45^\circ$.

cylinders is necessary for guided wave inspection of tubing and piping. Superposition of guided wave normal modes is useful in the theoretical analysis. Surface loading conditions, such as circumferential loading angles and axial loading lengths, can be used with the frequency and the phase velocity to control the axisymmetric and non-axisymmetric mode excitations. The experimental study demonstrates the use of a non-axisymmetric partial loading in generating axisymmetric modes in a sample Inconel tubing. 180° circumferential loading is almost as good as 360° axisymmetric loading, if we are interested only in a dominant axisymmetric mode. This non-axisymmetric excitation is particularly useful in the inspection application of tubing and piping with limited circumferential access. With circumferential loading angles of 90° and 45°, however, the axisymmetric modes are too weak for long distance axisymmetric field applications. The amount of flexural mode presence in a reflection from a defect potentially contains defect circumferential angle sizing information.

References

[1] D.C. Gazis, J. Acoust. Soc. Am. 31 (5) (1959) 568–573.
[2] D.C. Gazis, J. Acoust. Soc. Am. 31 (5) (1959) 573–578.
[3] J.E. Greenspon, J. Acoust. Soc. Am. 32 (5) (1960) 571–578.
[4] J.E. Greenspon, J. Acoust. Soc. Am. 32 (8) (1960) 1017–1025.
[5] A.H. Fitch, J. Acoust. Soc. Am. 35 (1963) 706–708.
[6] R.B. Thompson, R.K. Elsley, W.E. Peterson, C.F. Vasile, An EMAT system for detecting flaws in steam generator tubes, Ultrasonic Symposium (1979) 246–249.
[7] M.G. Silk, K.P. Bainton, Ultrasonics 17 (1979) 11–19.
[8] M. Brook, T.D.K. Ngoc, J. Eder, Ultrasonic inspection of steam generator tubing by chemical guided waves, in: D.O. Thompson, D.E. Chimenti (Eds.), Review of Progress in Quantitative Nondestructive Evaluation vol. 9, Plenum, New York, 1990, pp. 243–249.
[9] J.J. Ditri, J.L. Rose, G. Chen, Mode selection criteria for defect detection optimization using Lamb waves, D.O. Thompson, D.E. Chimenti (Eds.), Review of Progress in Quantitative Nondestructive Evaluation vol. 11, Plenum, New York, 1992, pp. 2109–2115.
[10] J.J. Ditri, J.L. Rose, A. Pilarski, Generation of guided waves in hollow cylinders by wedge and comb type transducers, Proceeding of the QNDE Conference vol. 12A (1993) 211–218.
[11] J.J. Ditri, J. Acoust. Soc. Am. 96 (1994) 3769–3775.
[12] J.L. Rose, J.J. Ditri, A. Pilarski, K.M. Rajana, F. Carr, NDTE International 27 (6) (1994) 307–310.

[13] J.L. Rose, K.M. Rajana, F.T. Carr, Materials Evaluation 52 (2) (1994) 307–311.
[14] H.J. Shin, R. Yi, J.L. Rose, Defect detection and characterization in power plant tubing using ultrasonic guided waves, 14th WCNDT, New Delhi, India, December 8–13, 1996.
[15] D.N. Alleyne, M. Lowe, P. Cawley, The inspection chemical plant pipework using lamb waves: defect sensitivity and field experience, in: D.O. Thompson, D.E. Chimenti (Eds.), Review of Progress in Quantitative Nondestructive Evaluation vol. 15, Plenum, New York, 1996, p. 1859.
[16] D.N. Alleyne, M. Lowe, P. Cawley, Journal of Nondestructive Evaluation 15 (1) (1996) 11–20.
[17] J.J. Ditri, J.L. Rose, J. Appl. Phys. 72 (7) (1992) 2589–2597.
[18] H.J. Shin, J.L. Rose, Journal of Nondestructive Evaluation 17 (1) (1998) 27–36.
[19] A.E. Armenakas, D.D. Gazis, G. Herrmann, Free Vibrations of Circular Cylindrical Shells, Pergamon, 1969.
[20] B.A. Auld, Acoustic Fields and Waves in Solids vol. II Wiley–Interscience, 1973.